Effects of land use on the concentration and emission of nitrous oxide in nitrogen-enriched rivers[☆]

Libiao Yang[*], Kun Lei

Estuarine and Coastal Environment Research Center, Chinese Research Academy of Environmental Sciences, Beijing, 100012, PR China

ABSTRACT

Nitrous oxide (N_2O) is a potent greenhouse gas that contributes to climate change and stratospheric ozone destruction. Nitrogen-enriched rivers are significant sources of atmospheric N_2O. This study conducted a one-year field campaign in seven N-enriched rivers draining urban, rural, and agricultural land to determine the link between the production, concentrations, and emissions of N_2O and land use. Estimated N_2O fluxes varied between 1.30 and 1164.38 μg N_2O-N m^{-2} h^{-1} with a mean value of 154.90 μg N_2O-N m^{-2} h^{-1}, indicating that rivers were the net sources of atmospheric N_2O. Concentrations of N_2O ranged between 0.23 and 29.21 μg N_2O-N L^{-1} with an overall mean value of 3.81 μg N_2O-N L^{-1}. Concentrations of ammonium and nitrate in urban and rural rivers were high in the cold season. The concentrations were also high in agricultural rivers in the wet season. N_2O concentrations and emissions in rural and urban rivers followed a similar pattern to ammonium and a similar pattern to nitrate in agricultural rivers. A strong link between the concentrations and emissions of N_2O and land use was observed. N_2O concentrations in and emissions from the rivers draining the urban and rural areas were significantly higher than the rivers draining the agricultural areas ($P < 0.01$). Stepwise regression analysis indicated that dissolved N_2O were primarily influenced by NH_4^+ in agricultural rivers and by NO_3^- in rural rivers; while dissolved N_2O in urban rivers was primarily predicted by temperature and reflected the integrated impact of sewage input and river hydrology. Nitrate-N and NO^{3-}-O isotope data and linear regression of N_2O and river water variables strongly indicated that dissolved N_2O was mainly derived from nitrification in agricultural rivers and denitrification in rural and urban rivers.

© 2018 Elsevier Ltd. All rights reserved.

1. Introduction

Nitrous oxide (N_2O) is an atmospheric trace gas and a strong ozone-depleting substance that has attracted considerable scientific attention (Garnier et al., 2009; Ravishankara et al., 2009). N_2O is the third most important greenhouse gas with a global warming potential approximately 298 times that of carbon dioxide (CO_2) over a 100-yr period (IPCC, 2013). Global nitrogen (N) enrichment has resulted in an increase in the concentration of atmospheric N_2O, which increased from ~270 parts per billion by volume (ppbv) in pre-industrial times to 321 ppbv at a rate of 0.25% yr^{-1} (IPCC, 2013). N_2O emissions are expected to remain at high levels throughout the 21st century and aquatic systems are estimated to contribute to 25%—30% of total global N_2O emissions (Ravishankara et al., 2009).

River systems receiving increased anthropogenic N loading from agricultural fertilizers and human waste are important sources of N_2O (Alvim et al., 2014; Seitzinger et al., 2000; Yan et al., 2012). High saturation and emission of N_2O has been measured from rivers in many studies globally (Seitzinger and Kroeze, 1998; Stow et al., 2005). Generally, riverine N_2O is produced as a byproduct of microbially mediated denitrification and nitrification. Under anaerobic conditions, denitrification can permanently remove nitrate-nitrogen (NO_3^--N), producing N_2O and N_2; annually; <1% of denitrified N is converted to N_2O (Beaulieu et al., 2010; Weier et al., 1993). Increased concentrations of NO_3^- may contribute to higher rates of denitrification and alter the ratio of N_2O to N_2 but may not increase the N_2O yield (Zhu et al., 2010). N_2O is also produced as a byproduct of nitrification where ammonium (NH_4^+) is oxidized to NO_3^- and N_2O under oxic conditions (Stein and Yung, 2003). Coupled nitrification—denitrification can be an important source of

N_2O in large, N-limited rivers (Allen et al., 2007; De Wilde and De Bie, 2000).

Thus, N_2O production is a function of both nitrification and denitrification. However, simple relationships between the rates of N cycling and N_2O production may not exist because of the uncertainty associated with spatial and temporal variations in environmental conditions. It is generally assumed that the dissolved inorganic nitrogen (DIN) load within a river is linearly related to riverine N_2O yield. However, this result seems to merit further study. Land use reflects the heterogeneity of a watershed and exerts a strong influence on river chemistry. The influence of land use categories on water parameters often varies with the spatial scale and seasons. Thus, biochemical processes of N in rivers also change with the heterogeneity of the watershed because of which riverine N_2O concentrations are linked to the land use (Harrison and Matson, 2003). Surface waters impacted by urbanization and anthropogenic activities exhibit individual hydrochemical characteristics; as a result, the factors controlling N_2O production and emissions may differ. Numerous investigations have found strong correlations between dissolved N_2O and NO_3^- concentrations in some agricultural or N-limited rivers (Harley et al., 2015; Herrman et al., 2008; Reay et al., 2003; Turner et al., 2016; Yan et al., 2012). However, the relationship between dissolved N_2O and nitrogen might be different in rural and urban rivers. A study by Wang et al. (2015a) found a significant positive relationship ($r^2 = 0.22$, $P < 0.001$) between NH_4^+ and N_2O production; NH_4^+ and dissolved oxygen (DO) explained 64% of the variability in N_2O production in urban rivers. Land use strongly affects water quality and sediment characteristics, which in turn enhance sediment denitrification and N_2O production (Garcia-Ruiz et al., 1998; Liu et al., 2015a). A study in a severely polluted urban river found that sediments were the sources of N_2O in river water (Wang et al., 2015b). Sediment denitrification in rivers can play an important role in riverine N_2O production; riverine N_2O concentration and emission dynamics vary greatly with the changes in land use. However, little is known about how N_2O changes with the land use type.

Understanding the linkage between the concentrations and emissions of riverine N_2O and land use can provide a scientific reference for establishing an inventory of greenhouse gases and land use management. This study reports the results of a 12-month investigation of seven N-enriched tributaries (including urban, rural, and agricultural rivers) in the Chao Lake basin, which is ideal for the purpose of this study because of the heavy water pollution and diversity of land use types in the basin. The objective of this study is to understand the effect of land-use on the seasonal dynamics of riverine N_2O concentrations and emissions.

2. Materials and methods

2.1. Site description

This research was conducted in the Chao Lake basin (E116°30′20″-118°0′0″, N30°58′40″−32°6′0″) in southeastern China with a watershed area of 13,500 km². This basin is located in a typical subtropical monsoon area. The annual average rainfall, wind speed, and temperature of this basin are 1100 mm, 3.5 m s^{-1}, and 18.8 °C, respectively. The rainy season is generally from June to August (Zhou and Wu, 2009).

The Chao Lake basin is one of the most densely populated areas in China, with a population of 61 million people. With local and regional development, N loading of the basin has increased continuously. Annually, approximately 1.2 billion tons of sewage enters the basin's urban rivers. This basin is also typical of agricultural production areas in central China, which are subject to heavy agricultural activity. Chemical fertilizers have been used

extensively in agricultural lands in recent years with a mean N fertilizer rate of 960 kg km^{-2} yr^{-1} across the Chao Lake basin; as a result, about 1900 tons of N leached to the rivers from various sources. Consequently, water quality in this basin has degraded substantially and the basin waterways are known to experience eutrophication and algal blooms.

Nutrient concentrations vary greatly among the tributaries flowing into the Chao Lake due to the differences in land use and human activities. In this study, seven major tributaries, the Nanfei (NR), Ershibu (ER), Dianbu (DR), Shiwuli (SR), Pai (PR), Fengle (FR), and Hangbu (HR) rivers were investigated (Fig. 1) and one sampling site was set up on each river. Rivers were categorized as urban, rural, and agricultural rivers according to the land-use type. In this study, agricultural rivers refer to the rivers that drain cropland areas; in those rivers, nutrients are mainly derived from surface runoff. Rural rivers drain populated areas in villages and towns and nutrients are mainly derived from the effluent of rural domestic sewage. Because the urban areas are larger, N concentrations in urban rivers could vary greatly between upper and lower reaches. To collect the representative water samples from urban rivers where sewage is well mixed with river water, the sampling sites in NR and ER are located in the downriver section and in city proper (Hefei City). Sampling sites in SR, DR, and PR were located in rural areas and sites in FR and HR in cropland areas (mainly for rice cultivation). The categories of land use for each river watershed are obtained via remote sensing and GIS (Table 1).

Based on the land-use data in Table 1, the percentages of developed land around the Nanfei, Ershibu, Shiwuli, and Dianbu rivers are close to each other (Table 1). The Nanfei and Ershibu rivers are classified as urban rivers, while Shiwuli and Dianbu rivers are classified as rural rivers. The developed land involves both urban and rural built-up areas. Although the percentages of developed land are close to each other, the Nanfei and Ershibu rivers (especially the sampling sites on those two rivers) are mainly located in urban areas (Hefei City) and the Shiwuli and Dianbu rivers are mainly located in rural areas (Cuozhen and Longtang).

2.2. Sample collection and chemical analysis

Monthly sampling to measure dissolved N_2O, water quality parameters, and abundance of nitrate isotopes was conducted from January to December 2013. Triplicate samples of surface river water were collected at a depth of 0.2 m using a water sampler. In the field, collected water samples were filtered through glass fiber filters (0.45 μm) and stored in acid-washed plastic bottles before the measurement of NH_4^+, NO_3^-, TP, BOD_5, COD_{Mn}, SO_4^{2-}, Cl^-, $\delta^{15}N$-NO_3^-, and $\delta^{18}O$-NO_3^- in the laboratory. DO, pH, and water temperature were measured *in situ* using a portable meter (HQ30D, U.S.). Other chemical analyses were conducted based on the standard methodology. The concentrations of NH_4^+, NO_3^-, TP, BOD_5, COD_{Mn}, SO_4^{2-}, and Cl^- were measured using an indophenol blue colorimetric method, an ultraviolet spectrophotometry method, an alkaline potassium persulfate digestion method, a dilution inoculation method, a standard titrimetric method, a gravimetric method, and mercury nitrate titration, respectively.

Samples were collected in serum bottles (60 mL, FIS#06-406H) tightly sealed with butyl-rubber stoppers to determine dissolved N_2O and preserved with the addition of a few drops of saturated mercuric chloride solution to prevent biological activity (Kirkwood, 1992). Samples were stored in a cooler during transport and analyzed within 24 h. The headspace-equilibrium method was used to measure the initial dissolved N_2O concentrations in river water (Clough et al., 2007; Crill et al., 1995; Huttunen et al., 2002). Then, 20 mL of highly purified N_2 (purity > 99.999%) was injected into the sampling bottle using an air-tight syringe and 20 mL of the water
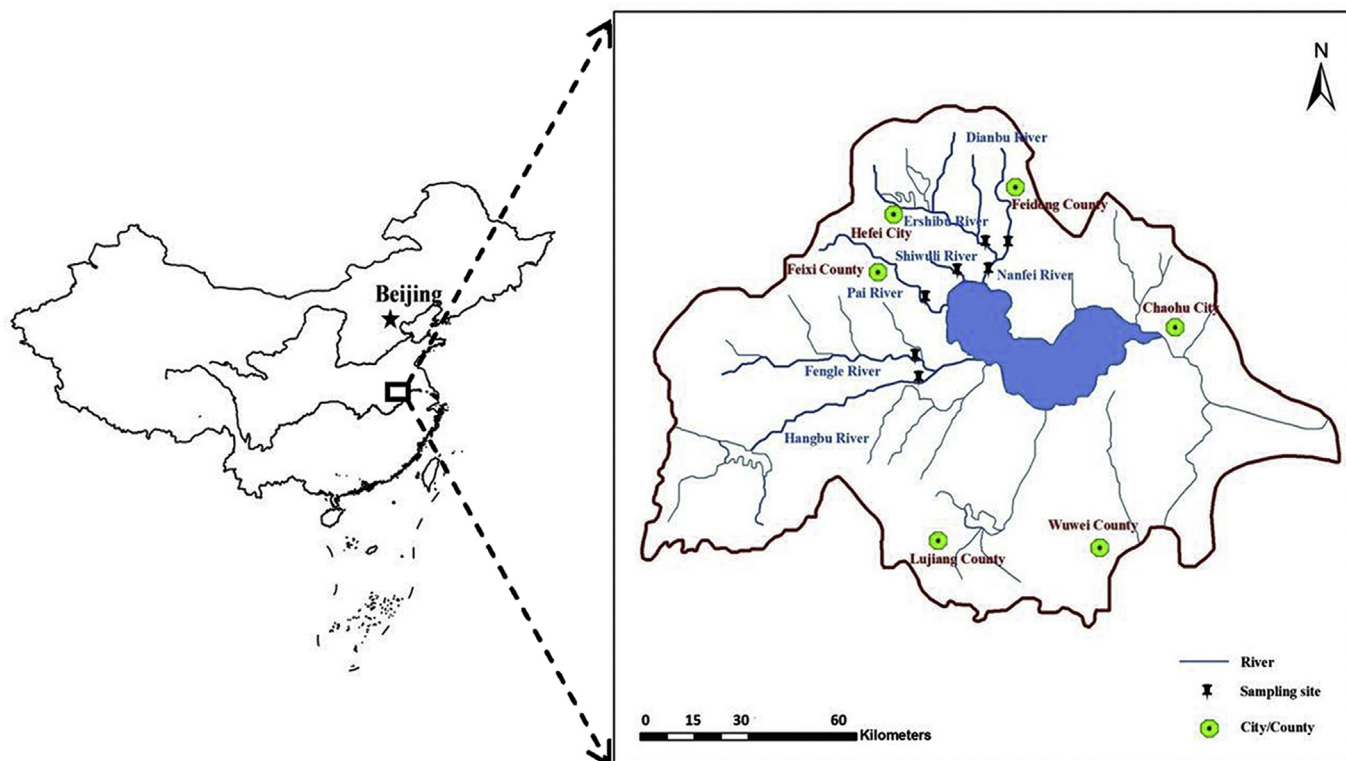
Fig. 1. Location of sampling sites of this study.

Table 1
Land uses of river watersheds.

River		Developed land (%)	Farmland (%)	Forests (%)	Water (%)
Urban rivers	Nanfei River	85	2	10	3
	Ershibu River	83	10	5	2
Rural rivers	Shiwuli River	80	12	5	3
	Dianbu River	80	10	5	5
	Pai River	58	9	25	8
Agricultural rivers	Fengle River	10	70	10	10
	Hangbu River	10	72	5	13

sample was displaced. Dissolved N_2O concentrations were determined using a gas chromatograph (HP5890 II), equipped with an ECD (electron capture detector) operating at $350\,°C$ and a 2-m Porapak $80-100$ Q Column. The column oven temperature was $35\,°C$ and the carrier gas was N_2 with a flow rate of $30\,mL\,min^{-1}$ (Wang et al., 2007).

A denitrifier method was used to determine the nitrogen and oxygen isotopic compositions of NO_3^- in water samples. First, sample nitrate was quantitatively converted to N_2O by cultured denitrifying bacteria that lacked the active N_2O-reductase enzyme. Then, N_2O gas was automatically extracted, purified, and analyzed online using trace gas-isotope ratio mass spectrometry (IRMS). $\delta^{15}N$-NO_3^- and $\delta^{18}O$-NO_3^- of the produced N_2O were measured on an IsoPrime100 stable isotope ratio mass spectrometer with a trace gas system connected to a Gilson auto sampler using He as a carrier gas. During the measurement of $\delta^{15}N$, USGS34 potassium nitrate (KNO_3, $\delta^{15}N = -1.8 \pm 0.2‰$) and USGS32 KNO_3 ($\delta^{15}N = 180 \pm 1‰$) standards were used as reference materials. For the $\delta^{18}O$ measurement, the samples were referenced using USGS34 ($\delta^{18}O = 27.9 \pm 0.6‰$) and USGS35 sodium nitrate ($NaNO_3$, $\delta^{18}O = 57.5 \pm 0.6‰$) standards (Xu et al., 2012).

2.3. Calculation of N_2O flux

N_2O flux across the water-air interface was estimated using the following equation:

$$F = k \times (C_m - C_e) \tag{1}$$

where F ($\mu g\ N_2O$-N $m^{-2}\ h^{-1}$) is the gas flux, positive numbers indicate a net flux from the river water to the atmosphere; C_m ($nmol\ L^{-1}$) and C_e ($nmol\ L^{-1}$) are the measured and equilibrium concentrations of N_2O, respectively; k ($cm\ h^{-1}$) is the gas transfer coefficient. In this study, k was calculated using the following empirical equation accounting for both wind speed and water flow rate (Borges et al., 2004):

$$k = \left[1.0 + 1.719(w/h)^{0.5} + 2.58\mu_{10}\right](S_c/600)^{-1/2} \tag{2}$$

where w ($m\ s^{-1}$) and h (m) are the river water velocity and river depth, respectively; μ_{10} ($m\ s^{-1}$) is the wind speed at a height of 10 m; Sc is the Schmidt number for N_2O, calculated using the equation of Wanninkhof (1992) at *in situ* temperature. In this study,

the percent saturation of dissolved N_2O was calculated as the ratio of the measured and the equilibrium concentrations determined by the solubility equation (Weiss and Price, 1980). Wind speed data were acquired from the Hefei Meteorological Bureau. To calculate the N_2O flux, we used the instantaneous wind speed at the sampling time measured at the nearby meteorological observation tower. Water discharge, velocity and depth of rivers were measured by a using an Acoustic Doppler Current Profiler (ADCP).

The values of k were estimated using different models. Widely used models of k are based on the empirical relationships linked to the wind speed (e.g., Wanninkhof, 1992). However, there is an ongoing debate on how to best predict the k value for a specific site because many processes that affect k values are not only related to wind forcing. Ten commonly used models were selected to examine the reliability of the riverine N_2O flux by comparing the results of all models (Table 2).

2.4. Statistical analysis

The SPSS software package (Version 17.0, SPSS Inc., U.S.) was used for all statistical analyses. The normality of data was tested before running the statistical analysis. The N_2O concentrations, flux, and NH_4^+ and NO_3^- concentrations were not normally distributed. Thus, significance tests between groups were performed using the Kruskal-Wallis method. The Spearman correlation analysis was carried out to detect the relationships between water parameters, $\delta^{15}N\text{-}NO_3^-$, and $\delta^{18}O\text{-}NO_3^-$. Simple linear regression was performed to determine the relationships between the N_2O and nutrient concentrations and stepwise regression was conducted to assess the predictors of N_2O concentrations in the rivers after data were log transformed.

3. Results

3.1. Patterns of river variables

River flow and water discharge of seven rivers ranged from 0.04 to 0.79 $m\,s^{-1}$ (average = 0.2 $m\,s^{-1}$) and from 1.5 to 330 $m^3\,s^{-1}$ (average = 34.1 $m^3\,s^{-1}$) (Fig. 2), respectively. The maximum river flow and water discharge occurred in July. The Nanfei, Hangbu, and Fengle rivers exhibited greater discharge than the other rivers owing to their greater water depth and river width.

The concentration of surface water nutrients varied significantly among rivers and over time. Overall, monthly concentrations of NH_4^+-N, NO_3^--N, and TP ranged from 0.1 to 32.1, from 0.01 to 17.9, and from 0.04 to 3.4 $mg\,L^{-1}$, respectively. According to the classification of water quality by the Chinese government ("Environmental Quality Standards for Surface Water"), the water quality of the studied rivers is classified as Grade III—V, suggesting that they are not safe to use as drinking water. Concentrations of NH_4^+-N and NO_3^--N in urban rivers were significantly higher than the rural and

agricultural rivers (Fig. 3). DO concentrations ranged from 0.2 $mg\,L^{-1}$ to 14.7 $mg\,L^{-1}$ with an annual mean value of 3.8 $mg\,L^{-1}$. In contrast, DO concentrations were typically higher in agricultural rivers (mean 6.3 $mg\,L^{-1}$) than in urban (mean 2.6 $mg\,L^{-1}$) and rural (mean 3.0 $mg\,L^{-1}$) rivers. In rural rivers, we found a negative correlation between DO and NH_4^+-N and a positive correlation between DO and NO_3^--N. However, DO was not significantly correlated with NH_4^+-N or NH_4^+-N in urban and agricultural rivers. By pooling all the data, we found that DO was negatively correlated with NH_4^+-N.

During the sampling period, concentrations of BOD_5 and COD_{Mn} ranged from 0.80 $mg\,L^{-1}$ to 38.5 $mg\,L^{-1}$ and from 3.3 $mg\,L^{-1}$ to 22.1 $mg\,L^{-1}$, respectively, with the highest concentration observed in the rural rivers. The concentrations of Cl^- and SO_4^{2-} ranged from 2.69 $mg\,L^{-1}$ to 277.14 $mg\,L^{-1}$ and from 11.5 $mg\,L^{-1}$ to 726.2 $mg\,L^{-1}$, respectively. Concentrations of Cl^- and SO_4^{2-} in urban and rural rivers were significantly higher than in agricultural rivers. Chloride is a conserved ion in natural water and thus can be used to trace mixing. Cl^- was significantly negatively correlated with NH_4^+ in urban rivers, reflecting the mixing of the river and sewage water. Nutrient concentrations exhibited a consistent seasonal pattern; a significantly higher level of nutrients occurred during the dry season (October through March, $P < 0.01$).

3.2. Isotope composition of nitrate

The $\delta^{15}N\text{-}NO_3^-$ and $\delta^{18}O\text{-}NO_3^-$ levels in the water were determined for seven rivers. The N isotope values of NO_3^- ranged from 11.00‰ to 37.71‰ (average = 24‰) in urban rivers, from −22.26‰ to 35.22‰ (average = 8.26‰) in rural rivers, and from −3.30‰—10.89‰ (average = 6.42‰) in agricultural rivers (Fig. 4). The O isotope values of NO_3^- ranged from 2.52‰ to 75.17‰ (average = 21.09‰) in urban rivers, from −22.20‰ to 81.25‰ (average = 18.14‰) in rural rivers, and from −6.81‰ to 15.59‰ (average = 1.86‰) in agricultural rivers. Generally, $\delta^{15}N\text{-}NO_3^-$ and $\delta^{18}O\text{-}NO_3^-$ were significantly higher in urban rivers than in rural and agricultural rivers. We found a significant positive correlation between $\delta^{15}N\text{-}NO_3^-$ and $\delta^{18}O\text{-}NO_3^-$ in urban rivers ($R^2 = 0.38$, $P = 0.01$) and in rural rivers ($R^2 = 0.53$, $P < 0.001$). However, the correlation between $\delta^{15}N\text{-}NO_3^-$ and $\delta^{18}O\text{-}NO_3^-$ was not significant in agricultural rivers ($R^2 = 0.10$, $P = 0.23$).

3.3. Dissolved N_2O concentrations and efflux

Dissolved N_2O ranged between 0.23 and 29.21 $\mu g\,N_2O\text{-}N\,L^{-1}$ in all river samples, with an overall mean concentration of 3.81 $\mu g\,N_2O\text{-}N\,L^{-1}$ (Fig. 5). Dissolved N_2O was supersaturated with respect to atmospheric equilibrium concentrations, ranging between 124% and 12,084% (mean 1467%). The maximum N_2O concentration was observed at NR in November. Repeated measures analysis showed that N_2O concentrations varied significantly with time ($P = 0.001$) and showed a clear seasonal trend over the

Table 2
Empirical equations for gas transfer coefficients.[a]

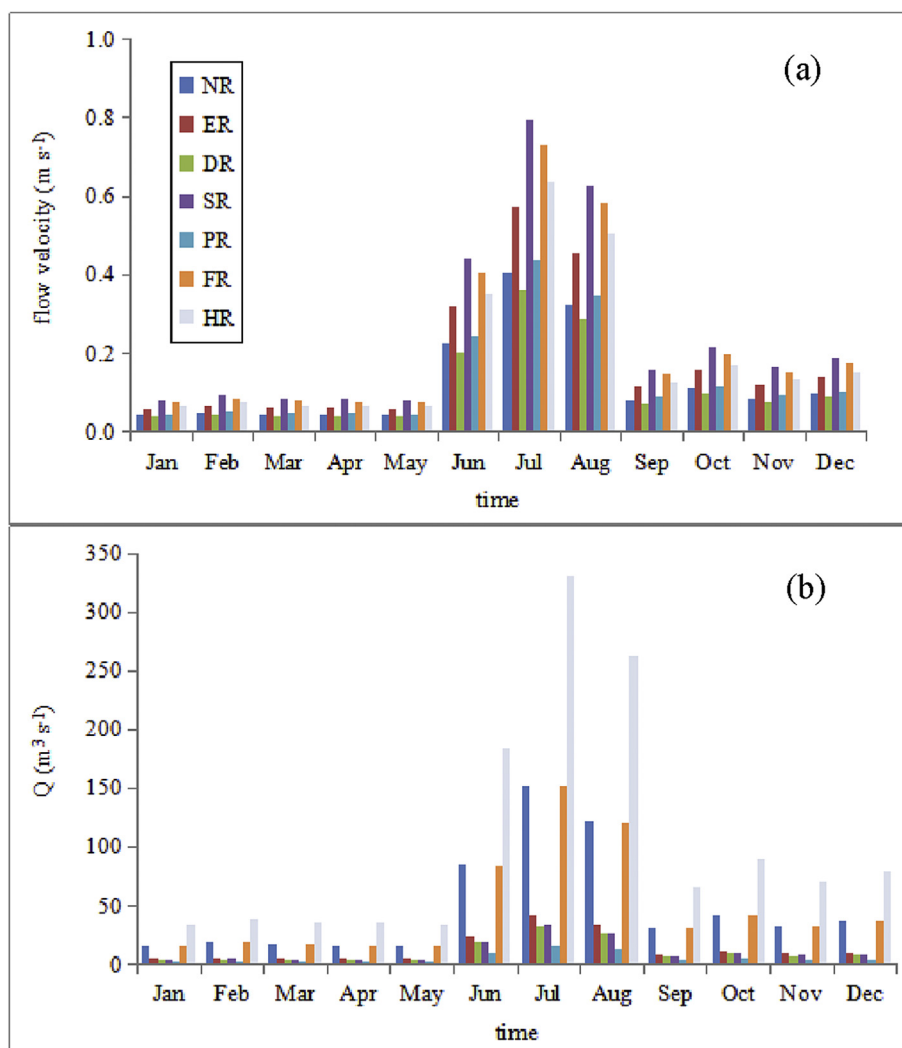| Model	Equation for k_{N2O} (cm h^{-1})	U_{10} (m s^{-1})	Reference
LM86a	$k_{N2O} = 0.17U_{10}(Sc/600)^{-2/3}$	$0 < U_{10} \leq 3.6$	Liss and Merlivat (1986)
LM86b	$k_{N2O} = (2.85 \times U_{10}\text{-}9.65)(Sc/600)^{-1/2}$	$3.6 < U_{10} \leq 13$	
W92a	$k_{N2O} = 0.39\,U_{10}^2(Sc/660)^{-1/2}$	Long-term U_{10}	Wanninkhof (1992)
W92b	$k_{N2O} = 0.31\,U_{10}^2(Sc/660)^{-1/2}$	Short-term U_{10}	
BO04	$k_{N2O} = (1.0 + 1.719w^{1/2}h^{-1/2} + 2.58U_{10})(Sc/600)^{-1/2}$		Borges et al. (2004)
Ma95	$k_{N2O} = 0.45U_{10}^{1.6}(Sc/600)^{-1/2}$		MacIntyre and Chanton (1995)
UG90	$k_{N2O} = 1.11U_{10} + 0.35$	$U_{10} < 9.5\pm3$	Upstill-Goddard et al. (1990)
WB91	$k_{N2O} = 0.32U_{10}^{1.73}$		Wanninkhof and Bliven (1991)
CL07	$k_{N2O} = 17.19w^{1/2}h^{-1/2} + 0.31U_{10}^2(Sc/600)^{-1/2}$		Clough et al. (2007)
RC01	$k_{N2O} = 1.91\exp(0.35U_{10})(Sc/600)^{-1/2}$		Raymond and Cole (2001)

Fig. 2. Monthly river flow velocity and discharge of the rivers.

sampling period. Overall, the temporal analysis showed that the N_2O concentrations in spring (mean $= 6.05 \, \mu g \, N_2O\text{-}N \, L^{-1}$) and winter (mean $= 5.43 \, \mu g \, N_2O\text{-}N \, L^{-1}$) were significantly higher than in summer (mean $= 1.46 \, \mu g \, N_2O\text{-}N \, L^{-1}$) and fall (mean $= 2.32 \, \mu g \, N_2O\text{-}N \, L^{-1}$) (one-way ANOVA, LSD, $P < 0.01$). There was a significant correlation between N_2O concentrations and time ($R^2 = 0.8099$, $P < 0.05$). In addition, N_2O concentrations in urban rivers (mean $= 7.08 \, \mu g \, N_2O\text{-}N \, L^{-1}$) were significantly higher than in rural (mean $= 3.36 \, \mu g \, N_2O\text{-}N \, L^{-1}$) and agricultural (mean $= 0.84 \, \mu g \, N_2O\text{-}N \, L^{-1}$) rivers (one-way ANOVA, LSD, $P < 0.01$).

We also tested the correlations between N_2O concentrations and land-use data by category for each river watershed. The results showed that dissolved N_2O concentrations in urban and rural rivers were significantly positively related to the proportion of developed land in a watershed ($R^2 = 0.3253$, P < 0.05) (Fig. 5). In agricultural rivers, the proportion of farmland (72%) in the HR watershed was higher than in FR (70%). The mean N_2O concentration in HR ($0.99 \, \mu g \, N_2O\text{-}N \, L^{-1}$) was also higher than in FR ($0.69 \, \mu g \, N_2O\text{-}N \, L^{-1}$). Thus, N leaching from the farmland likely plays a primary role in N_2O concentrations in agricultural rivers.

N_2O fluxes ranged from 1.30 to $1164.38 \, \mu g \, N_2O\text{-}N \, m^{-2} \, h^{-1}$ with an overall mean of $154.90 \, \mu g \, N_2O\text{-}N \, m^{-2} \, h^{-1}$. As with N_2O concentrations, temporal variations in N_2O fluxes were pronounced

and a significant correlation between the N_2O flux and time was observed ($R^2 = 0.7698$, $P < 0.05$). N_2O flux was disproportionately high in winter and spring; about 77% of the N_2O flux occurred in spring and winter. For example, N_2O flux from NR was nearly 200 times greater in winter than in summer. N_2O fluxes from urban and rural rivers were significantly higher than those in agricultural rivers (one-way ANOVA, LSD, $P < 0.01$).

The comparison of N_2O transfer coefficients estimated using the selected models is shown in Fig. 6. Overall, significant differences in estimated transfer coefficients (1.5−17.0 fold) were found between the models. LM86a always produced the lowest k value ($0.22-0.47 \, cm \, h^{-1}$, mean $= 0.36$), whereas CL07 showed the highest k value ($1.23-29.05 \, cm \, h^{-1}$, mean $= 10.87$). Model BO04 showed intermediate k_{N2O} values ($2.37-8.31 \, cm \, h^{-1}$, mean $= 4.61$) compared to other selected models, indicating that the estimated N_2O fluxes from the study rivers were within reasonable ranges.

4. Discussion

4.1. Sources and transformation of riverine N

The N in rivers originates from various sources, including surface runoff, chemical fertilizers, wastewater, and animal manure. N and
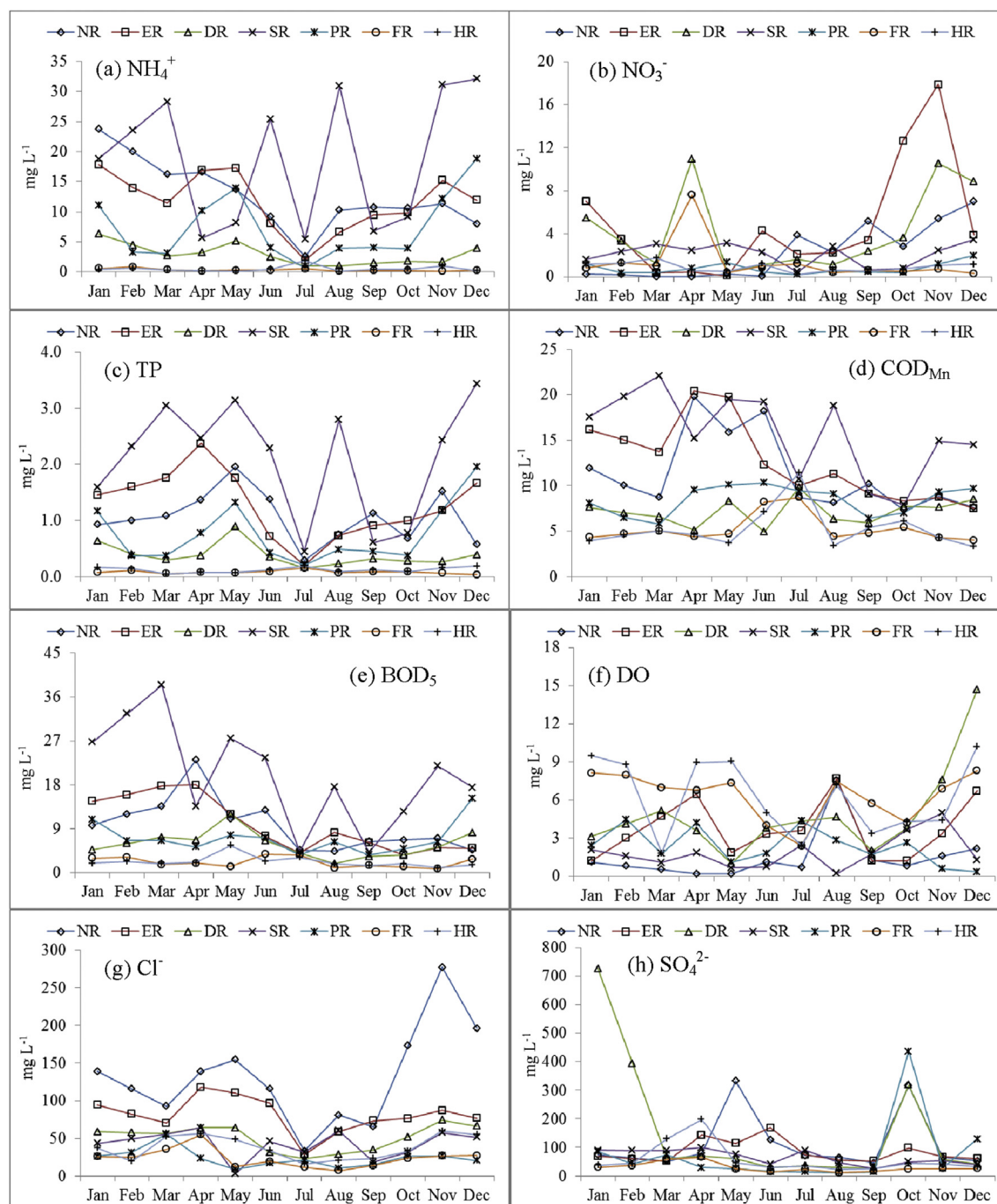
Fig. 3. Seasonal variation of river water chemistry.

O isotopes of nitrate from different sources have specific ranges of values (Anderson and Cabana, 2005; Bardhan et al., 2015). Thus, dual isotopes in nitrate are useful to identify the sources and transformation of N. Generally, most of the N isotopic values (Fig. 4) fall in the box identifying the isotopic composition of various N sources (Kendall et al., 2007; Xue et al., 2009).

The N isotope composition in water samples within the Chao Lake basin have been studied previously. Liu et al. (2012) found that N isotope values in industrial discharge, human sewage, and agriculture runoff ranged from 17.90‰ to 20.30‰, from 10.10‰ to 19.00‰, and from 8.1‰ to 10‰, respectively. The N isotope values of NO_3^- in river water samples had a similar pattern. Thus, by

combining those results with our analysis of the N isotope data (Fig. 4), we conclude that the NO_3^- in urban and rural rivers in this study mainly originated from industrial and human sewage discharge. In contrast, NO_3^- in PR (a rural river) may be greatly impacted by the effluence of wastewater from a nitrogen fertilizer plant located upstream of the sampling site. $\delta^{15}N\text{-}NO_3^-$ values in FR and HR were within the expected range of soil organic N and would resemble a mixture of soil mineralization and nitrification of NH_4^+ fertilizer. In addition, high $\delta^{18}O\text{-}NO_3^-$ (>60‰) were always detected during the high flow season, highlighting the impact of precipitation on N and O isotope composition.

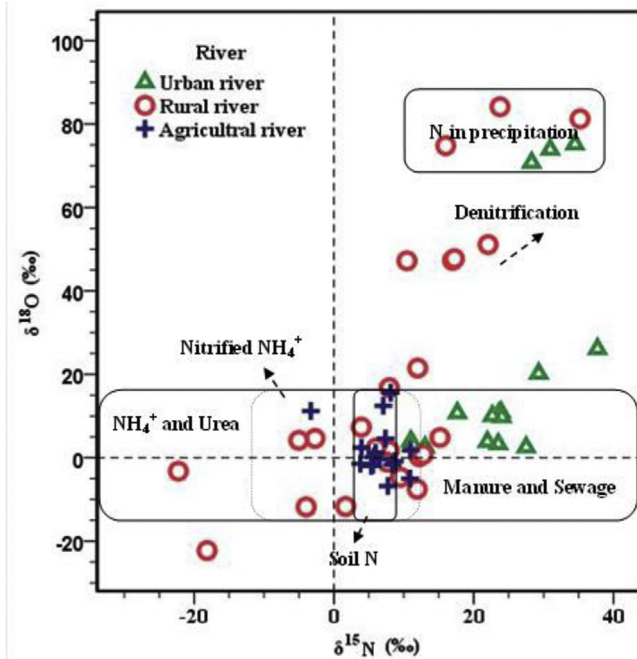Denitrification is an important mechanism for the reduction of

Fig. 4. N sources in river water identified by the isotopic composition in NO_3^- (Kendall et al., 2007; Xue et al., 2009).

Fig. 6. Comparison of gas transfer coefficients estimated using different models. K_{N2O} was estimated with LM86-Liss and Merlivat (1986), W92-Wanninkhof (1992), BO04-Borges et al. (2004), Ma95-MacIntyre and Chanton (1995), UG90-Upstill-Goddard et al. (1990), WB91-Wanninkhof and Bliven (1991), CL07-Clough et al. (2007), and RC01-Raymond and Cole (2001). The box shows the 10th, 90th, 25th, and 75th percentiles, maximum, mean, and minimum values. Each box in the figure was plotted using all the observed data of the study. The model selected to estimate N_2O fluxes in our study was marked with a grey shape.

the NO_3^- load in aquatic environments and usually causes isotopic enrichment of residual NO_3^- (Böttcher et al., 1990). In this study, significant denitrification affected the NO_3^- distribution in the rural and urban river water because a significant positive correlation
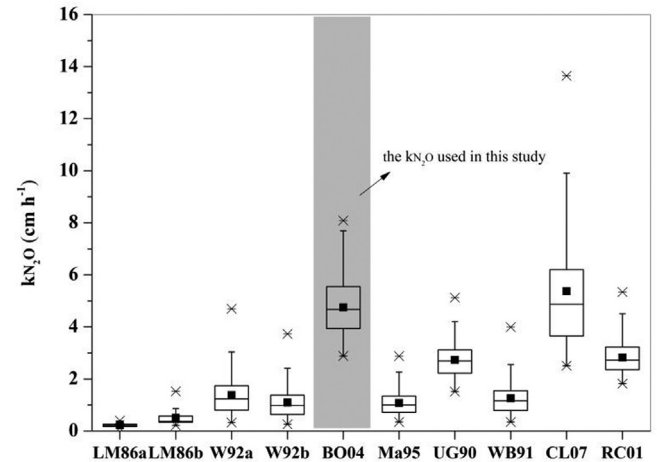
between $\delta^{15}N-NO_3^-$ and $\delta^{18}O-NO_3^-$ was found in these rivers (Yue et al., 2013). However, high concentrations of dissolved O_2 (mean 6.3 mg L^{-1}) in agricultural rivers indicated that there was minimal denitrification.

The molar ratio of N_2O/NO_3^- in rivers could help to determine the percentage of N_2O that is lost from each N source and the effect

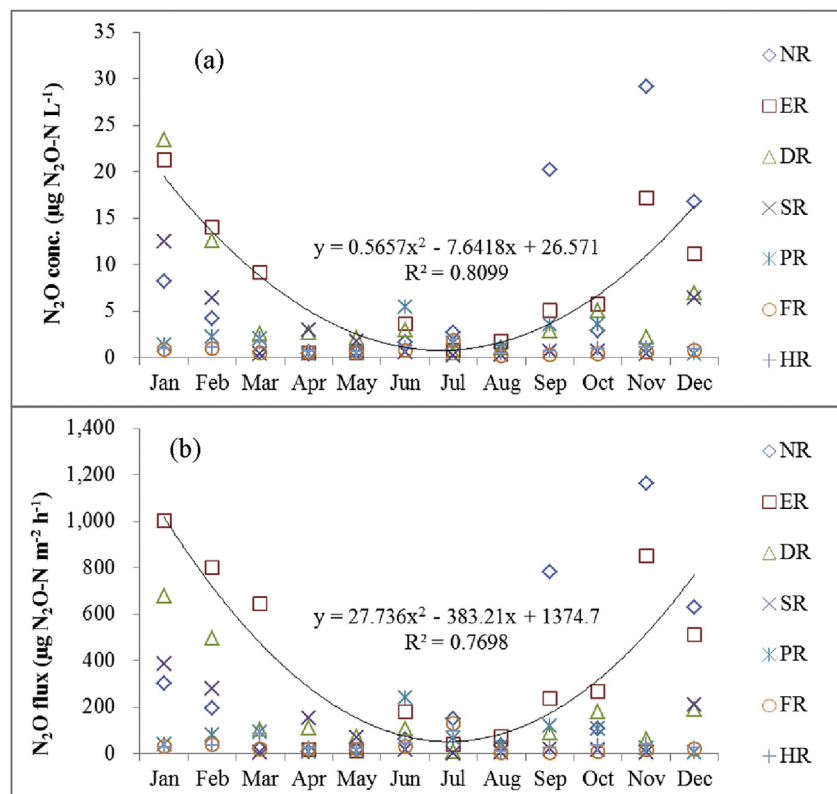**Fig. 5.** Seasonal variations of N_2O concentrations and fluxes.

of the type of N input on N_2O flux. In this study, the molar ratio of N_2O/NO_3^- in urban, rural, and agricultural rivers ranged between 0.17% and 15.71%, 0.10% and 18.92%, and 0.03% and 4.07%, with mean values of 3.08%, 1.84%, and 0.59%, respectively. A greater percentage of NO_3^- was transformed to N_2O and lost to the atmosphere in urban and rural rivers, indicating that these rivers received sewage effluence and are significant sources of atmospheric N_2O. The high ratio of N_2O/NO_3^- and positive relationship between $\delta^{15}N$-NO_3^- and $\delta^{18}O$-NO_3^- strongly indicate that denitrification is the main driver of N_2O production in urban and rural rivers.

4.2. Patterns of N_2O concentration and efflux

N_2O concentrations and emissions observed in urban and rural rivers were significantly higher than in agricultural rivers. This pattern may be caused by the variations in N loading among the rivers. Many studies have demonstrated that river water with high N loading and concentrations has higher N_2O concentrations and emissions (Beaulieu et al., 2010).

In this study, dissolved N_2O in urban and rural rivers was high in winter and spring, but the highest N_2O concentrations in agricultural rivers were observed in summer (Fig. 5). The higher concentrations of N_2O in summer in agricultural rivers may be a result of the increased N leaching from intensive agricultural activities on farmlands and precipitation. Hinshaw and Dahlgren (2013) also reported that the concentrations of N_2O were the highest in late fall and early summer and lowest in winter in agriculturally impacted rivers (e.g., San Joaquin River). Generally, N_2O production is stimulated at high temperatures (Seitzinger, 1988), but significant N_2O production can occur at low temperatures (Wagner-Riddle et al., 2017). In this study, the higher N_2O concentrations in winter in urban and rural rivers might be a result of the integrated impact of N input and river hydrology. N_2O concentrations in urban and rural rivers could be highly impacted by the direct input of N_2O from sewage. This influence was especially significant in the cold season due to the lower river discharge and reduced precipitation. In this study, a significant negative correlation between the river

discharge and N concentrations was detected in urban and rural rivers ($P < 0.01$). Since the Chao Lake basin is located in a typical subtropical monsoon area with an annual mean temperature of 18.8 °C, the production rates of N_2O during winter and spring may not be substantially inhibited by temperature but may be accelerated by increased N concentrations.

The N_2O fluxes showed a similar pattern to dissolved N_2O concentrations. N_2O emissions from seven rivers were greatly controlled by dissolved N_2O concentrations. This is different from the rivers in northern China that show significant seasonal fluctuations in water velocity and water depth. The rivers in this study are located in a subtropical humid monsoon climate zone and water depth of each river showed no obvious variations between the months. Water velocity of the seven rivers is very small because of the backwater of Lake Chaohu. Consequently, seasonal variations in k_{N2O} associated with wind speed, water depth, and water velocity in the rivers are less sensitive than N_2O concentrations. As a result, the seasonality of N_2O fluxes would be greatly controlled by $\Delta[N_2O]$; i.e., $Flux = k_{N2O} \times \Delta[N_2O]$.

4.3. Control of N_2O production

Simple linear regression showed N_2O concentrations in agricultural rivers to be positively correlated with NH_4^+ ($R^2 = 0.549$, $P < 0.0001$) and NO_3^- ($R^2 = 0.1277$, $P = 0.085$), and negatively correlated with DO ($R^2 = 0.2665$, $P = 0.0164$), indicating that aerobic nitrification could be responsible for the production of N_2O (Fig. 7). The relationship between N_2O concentrations and NH_4^+ was especially strong, suggesting that NH_4^+ could exert a much stronger control on N_2O production in agricultural rivers than NO_3^- or DO. In rural rivers, lower DO levels and a significant positive correlation between N_2O and NO_3^- concentrations ($R^2 = 0.2239$, $P = 0.0041$) suggest that the major source of N_2O is denitrification. In urban rivers, N_2O concentrations were not significantly correlated with DO, but significant positively correlated with NO_3^- ($R^2 = 0.3340$, $P = 0.0044$); i.e., N_2O production was mainly regulated by the coupled nitrification–denitrification process. Many studies showed that denitrification rate in sediment and N_2O flux across the
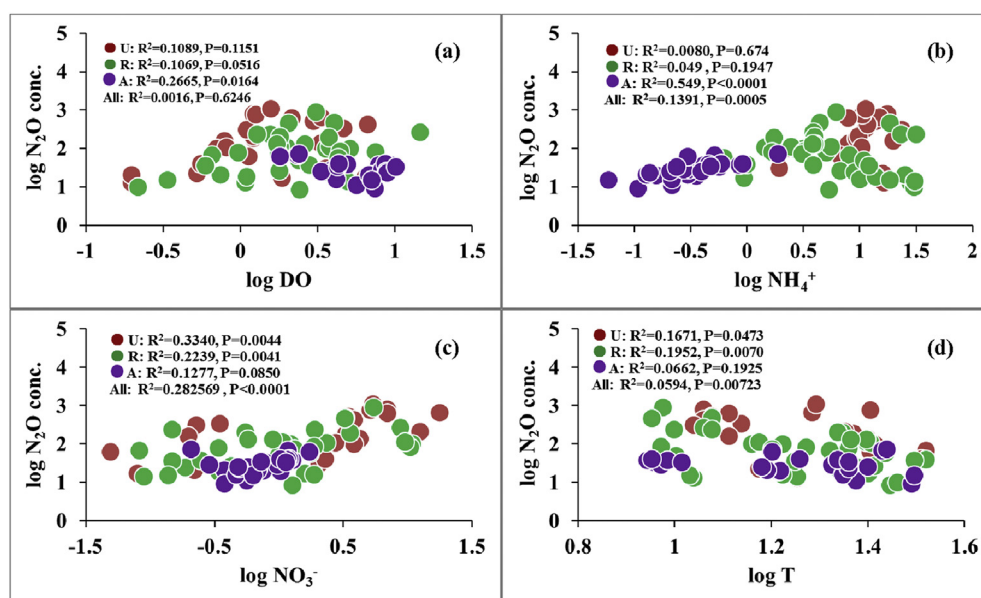

Fig. 7. Simple linear regression analysis of N_2O concentration with (a) DO, (b) NH_4^+, (c) NO_3^-, and (d) water temperature (T) for agricultural, rural, and urban rivers. The letters "A," "R," and "U" represent agricultural, rural, and urban rivers, respectively.

sediment-water interface are high under anaerobic conditions; correspondingly, sediment becomes a major source of dissolved N_2O in river waters (Liu et al., 2015b). We did not collect river sediment samples or simulate the contribution of sediment on dissolved N_2O in this study; however, the role of sediment in the concentration and production of N_2O cannot be ignored.

As reported by Harrison and Matson (2003), several environmental variables can together predict dissolved N_2O concentrations, but none of them individually acts as the best predictor of N_2O. The stepwise regression analysis was also conducted to assess the predictors of N_2O concentrations in the rivers. NH_4^+, NO_3^-, and COD_{Mn} explained 70% of the variation in N_2O concentrations in agricultural rivers; NH_4^+ and pH explained 41% of the variation in N_2O concentrations in rural rivers; and water temperature explained 43% of the variation in N_2O concentrations in urban rivers.

4.4. Uncertainties in emission estimations

A rigorous estimation of the N_2O flux across the air-water interface is critical to budgeting the sinks or sources of atmospheric N_2O. Attempts have been made to establish local, regional, and global riverine N_2O fluxes (Garnier et al., 2006; Rosamond et al., 2012; Syakila and Kroeze, 2011). However, there is still uncertainty surrounding these estimates, partially because of the errors in estimated gas transfer coefficients (k) (Cicerone and Oremland, 1988; Nevison et al., 1995). Physical processes (tidal currents, rain, surfactants, wave fetch) regulating turbulence have great effects on the rate of gas transfer. Thus, some researchers have proposed a model for predicting k using the turbulent dissipation rate and river current in a variety of environmental conditions (Borges et al., 2004; Zappa et al., 2007). Gas transfer coefficients can also be obtained by the floating chambers method, which has some limitations; for example, the chamber disturbs the surface wind boundary layer, invalidating the measured k values (Liss and Merlivat, 1986). As a result, using only the wind and current model to estimate k in rivers may grossly underestimate N_2O emissions (Duchemin et al., 1999).

In this study, model BO04 (Table 2) was used to estimate the N_2O flux. The estimated N_2O fluxes from the study rivers were reasonable (Fig. 6). Emissions obtained using only k_{wind} for the study period were lower than the emissions obtained using k_{wind} and $k_{currents}$ models and the differences in k_{N2O} among the models can cause variation of up to an order of magnitude in the estimated fluxes. This is because the models were developed in different environmental settings and gas transfer coefficients from the water surface estimated using these models did not satisfy all field conditions (Borges et al., 2004; Upstill-Goddard, 2006). Consequently, further efforts, particularly *in situ* tracer studies to scale the measured k values, are necessary for improving riverine N_2O emissions in the future.

5. Conclusions

This study showed that rivers receiving anthropogenic N inputs are strong sources of atmospheric N_2O. Concentrations and emissions of N_2O varied in rivers located in watersheds with different land uses. Dissolved N_2O concentrations in urban rivers receiving domestic or industrial wastewater were significantly higher than in agricultural and rural rivers ($P < 0.01$). Based on the pooled data, dissolved N_2O linearly increased with NO_3^- concentrations ($R^2 = 0.312$, $P < 0.001$). However, NH_4^+ and DO levels exerted considerable control over N_2O concentrations in the agricultural and rural rivers, respectively. N_2O concentrations in urban rivers may have been mainly controlled by direct N_2O input from industrial sewage. There was a pattern of seasonality in N_2O concentrations and emissions that resulted from the integrated impact of N loading and river hydrology. In urban and rural rivers, concentrations and emissions of N_2O were high in winter and spring, whereas in agricultural rivers the highest value was observed in summer.

References

Allen, D.E., Dalai, R.C., Rennenberg, H., et al., 2007. Spatial and temporal variation of nitrous oxide and methane flux between subtropical mangrove sediments and the atmosphere. Soil Biol. Biochem. 39, 622–631.

Alvim, R.B., de Mello, W.Z., Silveira, C.S., Kligerman, D.C., Ribeiro, R.P., 2014. Nitrous oxide emissions from unpolluted and polluted rivers of the Paquequer Basin (Teresopolis, Rio de Janeiro). Eng. Sanit. E Ambient. 19, 471–478.

Anderson, C., Cabana, G., 2005. $\delta^{15}N$ in riverine food webs: effects of N inputs from agricultural watersheds. Can. J. Fish. Aquat. Sci. 62 (2), 333–340.

Bardhan, P., Karapurkar, S.G., Shenoy, D.M., et al., 2015. Carbon and nitrogen isotopic composition of suspended particulate organic matter in Zuari Estuary, west coast of India. J. Mar. Syst. 141, 90–97.

Beaulieu, J.J., Tank, J.L., Hamilton, S.K., et al., 2010. Nitrous oxide emission from denitrification in stream and river networks. PNAS 108, 214–219.

Borges, A.V., Vanderborght, J.P., Schiettecatte, L.S., et al., 2004. Variability of the gas transfer velocities of CO_2 in a macrotidal estuary (the Scheldt). Estuaries 27, 593–603.

Böttcher, J., Strebel, O., Voerkelius, S., et al., 1990. Using isotope fractionation of nitrate-nitrogen and nitrate-oxygen for evaluation of microbial denitrification in a sandy aquifer. J. Hydrol. 114, 413–424.

Cicerone, R.J., Oremland, R., 1988. Biogeochemical aspects of atmospheric methane. Glob. Biogeochem. Cycles 8, 385–397.

Clough, T.J., Buckthought, L.E., Kelliher, F.M., et al., 2007. Diurnal fluctuations of dissolved nitrous oxide (N_2O) concentrations and estimates of N_2O emissions from a spring-fed river: implications for IPCC methodology. Glob. Change Biol. 13, 1016–1027.

Crill, P.M., Butler, J.H., Cooper, D.J., Novelli, P.C., 1995. Standard analytical methods for measuring trace gases in the environment. In: Matson, P.A., Harriss, R.C. (Eds.), Biogenic Trace Gases: Measuring Emissions from Soil and Water. Blackwell Science, London, UK, pp. 164–205.

De Wilde, H.P.J., De Bie, M.J.M., 2000. Nitrous oxide in the Schelde Estuary: production by nitrification and emission to the atmosphere. Mar. Chem. 69, 203–216.

Duchemin, E., Lucotte, M., Canuel, R., 1999. Comparison of static chamber and thin boundary layer equation methods for measuring greenhouse gas emissions from large water bodies. Environ. Sci. Technol. 33, 350–357.

Garcia-Ruiz, R., Pattinson, S.N., Whitton, B.A., 1998. Denitrification in river sediments: relationship between process rate and properties of water and sediment. Freshw. Biol. 39 (3), 467–476.

Garnier, J., Cébron, A., Tallec, G., et al., 2006. Nitrogen behaviour and nitrous oxide emission in the tidal Seine River estuary (France) as influenced by human activities in the upstream watershed. Biogeochemistry 77, 305–326.

Garnier, J., Billen, G., Vilain, G., et al., 2009. Nitrous oxide (N_2O) in the Seine river and basin: observations and budgets. Agric. Ecosyst. Environ. 133, 223–233.

Harley, J.F., Carvalho, L., Dudley, B., et al., 2015. Spatial and seasonal fluxes of the greenhouse gases N_2O, CO_2 and CH_4 in a UK macrotidal estuary. Estuar. Coast. Shelf Sci. 153, 62–73.

Harrison, J., Matson, P., 2003. Patterns and controls of nitrous oxide emissions from waters draining a subtropical agricultural valley. Glob. Biogeochem. Cycles 17, 1080.

Herrman, K.S., Bouchard, V., Moore, R.H., 2008. Factors affecting denitrification in agricultural headwater streams in Northeast Ohio, USA. Hydrobiologia 598, 305–314.

Hinshaw, S.E., Dahlgren, R.A., 2013. Dissolved nitrous oxide concentrations and fluxes from the Eutrophic San Joaquin River, California. Environ. Sci. Technol. 47, 1313–1322.

Huttunen, J.T., Väisänen, T.S., Hellsten, S.K., Heikkinen, M., Nykänen, H., Jungner, H., Niskanen, A., Virtanen, M.O., Lindqvist, O.V., Nenonen, O.S., Martikainen, P.J., 2002. Fluxes of CH_4, CO_2, and N_2O in hydroelectric reservoirs Lokka and Porttipahta in the northern boreal zone in Finland. Glob. Biogeochem. Cycles 16, 1–17.

IPCC, 2013. Climate Change 2013: the Physical Science Basis. Contribution of Working Group I to the Fifth Assessment Report of the Intergovernmental Panel on Climate Change.

Kendall, C., Elliott, E.M., Wankel, S.D., 2007. Tracing anthropogenic inputs of

nitrogen to ecosystems. In: Michener, R.H., Lajtha, K. (Eds.), Stable Isotopes in Ecology and Environmental Science, second ed. Blackwell, Oxford, pp. 375—449.

Kirkwood, D.S., 1992. Stability of solutions of nutrient salts during storage. Mar. Chem. 38, 151—164.

Liss, P.S., Merlivat, L., 1986. Air-sea gas exchange rates: introduction and synthesis. In: Buat-Ménard, P. (Ed.), The Role of Air-sea Exchange in Geochemical Cycling. Reidel, Dordrecht, The Netherlands, pp. 113—129.

Liu, S., Kong, F.X., Cai, Y.F., et al., 2012. Nitrogen stable isotope study on nitrate nitrogen pollution of four inflowing rivers of Lake Chaohu. J. Lake Sci. 24 (6), 952—956.

Liu, X.L., Bai, L., Wang, Z.L., Li, J., Yue, F.J., Li, S.L., 2015a. Nitrous oxide emissions from river network with variable nitrogen loading in Tianjin, China. J. Geochem. Explor. 157, 153—161.

Liu, W., Yao, L., Wang, Z., et al., 2015b. Human land uses enhance sediment denitrification and N_2O production in Yangtze lakes primarily by influencing lake water quality. Biogeosci. Discuss. 12, 6059—6070.

MacIntyre, R.W., Chanton, J., 1995. Trace gas exchange across the air water interface in freshwater and coastal marine environments. In: Matson, P., Harriss, R. (Eds.), Biogenic Trace Gases: Measuring Emissions from Soil and Water. Blackwell, pp. 52—97 (Chapter 3).

Nevison, C.D., Weiss, R.F., Erickson, D.J., 1995. Global oceanic emissions of nitrous oxide. J. Geophys. Res. 100, 15809—15820.

Ravishankara, A.R., Daniel, J.S., Portmann, R.W., 2009. Nitrous oxide (N_2O): the dominant ozone-depleting substance emitted in the 21st century. Science 326, 123—125.

Raymond, P.A., Cole, J.J., 2001. Gas exchange in rivers and estuaries: choosing a gas transfer velocity. Estuaries 24, 312—317.

Reay, D.S., Smith, K.A., Edwards, A.C., 2003. Nitrous oxide emission from agricultural drainage waters. Glob. Change Biol. 9 (2), 195—203.

Rosamond, M.S., Thuss, S.J., Schiff, S.L., 2012. Dependence of riverine nitrous oxide emissions on dissolved oxygen levels. Nat. Geosci. 5, 715—718.

Seitzinger, S.P., 1988. Denitrification in freshwater and coastal marine ecosystems: ecological and geochemical significance. Limnol. Oceanogr. 33, 702—724.

Seitzinger, S., Kroeze, C., 1998. Global distribution of nitrous oxide production and N inputs in fresh water and coastal marine ecosystems. Glob. Biogeochem. Cycles 12, 93—113.

Seitzinger, S.P., Kroeze, C., Styles, R.V., 2000. Global distribution of N_2O emissions from aquatic systems: natural emissions and anthropogenic effects. Chemosphere Glob. Change Sci. 2, 267—279.

Stein, L.Y., Yung, Y.L., 2003. Production, isotopic composition, and atmospheric fate of biologically produced nitrous oxide. Annu. Rev. Earth Planet. Sci. 31, 329—356.

Stow, C.A., Walker, J.T., Cardoch, L., et al., 2005. N_2O emissions from streams in the Neuse River Watershed, North Carolina. Environ. Sci. Technol. 39, 6999—7004.

Syakila, A., Kroeze, C., 2011. The global nitrous oxide budget revisited. Greenhouse Gas Meas. Manag. 1, 17—26.

Turner, P.A., Griffis, T.J., Baker, J.M., Lee, X., Crawford, J.T., Loken, L.C., et al., 2016. Regional-scale controls on dissolved nitrous oxide in the Upper Mississippi River. Geophys. Res. Lett. 43, 4400—4407.

Upstill-Goddard, R.C., 2006. Air-sea gas exchange in the coastal zone. Estuar. Coast. Shelf Sci. 70, 388—404.

Upstill-Goddard, R.C., Watson, A.J., Liss, P.S., et al., 1990. Gas transfer velocities in lakes measured with SF6. Tellus 42B, 364—377.

Wagner-Riddle, C., Congreves, K.A., Abalos, D., et al., 2017. Globally important nitrous oxide emissions from croplands induced by freeze-thaw cycles. Nat. Geosci. 10, 279—283.

Wang, D.Q., Chen, Z.L., Wang, J., Xu, S.Y., Yang, H.X., Chen, H., Yang, L.Y., Hu, L.Z., 2007. Summer-time denitrification and nitrous oxide exchange in the intertidal zone of the Yangtze Estuary. Estuar. Coast. Shelf Sci. 73, 43—53.

Wang, J.N., Chen, N.W., Yan, W.J., et al., 2015a. Effect of dissolved oxygen and nitrogen on emission of N_2O from rivers in China. Atmos. Environ. 103, 347—356.

Wang, D.Q., Tan, Y.J., Yu, Z.J., Li, Y.J., Chang, S.Q., Deng, H.G., et al., 2015b. Nitrous oxide production in river sediment of highly urbanized area and the effects of water quality. Wetlands 35, 1213—1223.

Wanninkhof, R., 1992. Relationship between wind speed and gas exchange over the ocean. J. Geophys. Res. 97 (C5), 7373—7382.

Wanninkhof, R., Bliven, L.F., 1991. Relationship between gas exchange, wind speed, and radar backscatter in a large wind-wave tank. J. Geophys. Res. 96 (C2), 2785—2796.

Weier, K.L., Doran, J.W., Power, J.F., et al., 1993. Denitrification and dinitrogen/ nitrous oxide ratio as affected by soil water, available carbon, and nitrate. Soil Sci. Soc. Am. J. 57, 55—73.

Weiss, R.F., Price, B.A., 1980. Nitrous oxide solubility in water and seawater. Mar. Chem. 8, 347—359.

Xu, C.Y., Li, Y.Z., Hao, W.P., et al., 2012. Analysis of nitrogen isotopic composition of nitrate in water by denitrifier method and trace gas/isotope ratio mass spectrometry. Chin. J. Anal. Chem. 40 (9), 1360—1365.

Xue, D.M., Botte, J., De Baets, B., et al., 2009. Present limitations and future prospects of stable isotope methods for nitrate source identification in surface- and groundwater. Water Res. 43, 1159—1170.

Yan, W., Yang, L., Wang, F., et al., 2012. Riverine N_2O concentrations, exports to estuary and emissions to atmosphere from the Changjing River in response to increasing nitrogen loads. Glob. Biogeochem. Cycles 26, GB4006.

Yue, F.J., Li, S.L., Liu, C.Q., et al., 2013. Using dual isotopes to evaluate sources and transformation of nitrogen in the Liao River, northeast China. Appl. Geochem. 36, 1—9.

Zappa, C.J., McGillis, W.R., Raymond, P.A., Edson, J.B., Hintsa, E.J., Zemmelink, H.J., Dacey, J.W.H., Ho, D.T., 2007. Environmental turbulent mixing controls on air-water gas exchange in marine and aquatic systems. J. Geophys. Res. 34, L10601.

Zhou, G.J., Wu, L.X., 2009. Land use change and its driver factor in Chaohu Lake basin. J. East China Inst. Technol. 32 (3), 265—270.

Zhu, G.B., Jetten, M.S.M., Kuschk, P., et al., 2010. Potential roles of anaerobic ammonium and methane oxidation in the nitrogen cycle of wetland ecosystems. Appl. Microbiol. Biotechnol. 86 (4), 1043—1055.